International Journal of Nanomedicine

Dovepress

open access to scientific and medical research

Open Access Full Text Article

ORIGINAL RESEARCH

Lactoferrin- and Dendrimer-Bearing Gold Nanocages for Stimulus-Free DNA Delivery to Prostate Cancer Cells

Jamal Almowalad, Partha Laskar, Sukrut Somani, Jitkasem Meewan, Rothwelle J Tate, Christine Dufès

Strathclyde Institute of Pharmacy and Biomedical Sciences, University of Strathclyde, Glasgow, G4 0RE, UK

Correspondence: Christine Dufès, Strathclyde Institute of Pharmacy and Biomedical Sciences, University of Strathclyde, Glasgow, G4 0RE, UK, Tel +44 1415483796, Fax +44 1415522562, Email C.Dufes@strath.ac.uk

Background: The use of gene therapy to treat prostate cancer is hampered by the lack of effective nanocarriers that can selectively deliver therapeutic genes to cancer cells. To overcome this, we hypothesize that conjugating lactoferrin, a tumor-targeting ligand, and the diaminobutyric polypropylenimine dendrimer into gold nanocages, followed by complexation with a plasmid DNA, would enhance gene expression and anti-proliferation activity in prostate cancer cells without the use of external stimuli.

Methods: Novel gold nanocages bearing lactoferrin and conjugated to diaminobutyric polypropylenimine dendrimer (AuNCs-DAB-Lf) were synthesized and characterized. Following complexation with a plasmid DNA, their gene expression, cellular uptake and anti-proliferative efficacies were evaluated on PC-3 prostate cancer cells.

Results: AuNCs-DAB-Lf was able to complex DNA at conjugate: DNA weight ratios 5:1 onwards. Gene expression was at its highest after treatment with AuNCs-DAB-Lf at a weight ratio of 10:1, as a result of a significant increase in DNA uptake mediated by the conjugate at that ratio in PC-3 cells. Consequently, the anti-proliferative activity of AuNCs-DAB-Lf-DNA encoding TNFα was significantly improved by up to 9-fold compared with DAB dendriplex encoding TNFα.

Conclusion: Lactoferrin-bearing dendrimer-conjugated gold nanocages are highly promising gene delivery systems for the treatment of prostate cancer.

Keywords: gold nanocages, lactoferrin, dendrimer, gene therapy, cancer targeting, transfection efficacy, prostate cancer

Introduction

Prostate cancer is currently the second most common cancer and the fifth-leading cause of cancer death in men, with approximately 1.4 million new cases diagnosed and 375,000 deaths recorded globally in 2020.[1] Despite the advancements in available treatments for this cancer, current therapy can only provide a short increase in lifespan and offers limited therapeutic effects for patients suffering from metastatic or recurrent diseases.[2] Consequently, novel and improved therapeutic strategies are urgently needed for treating these patients. Among innovative techniques, gene therapy offers promising potential for prostate cancer therapy. However, its application is currently hampered by the lack of safe and efficient vectors that can deliver therapeutic genes to tumors in a selective way, without causing side effects on healthy tissues. Gold nanocages are novel multimodal nanomaterials that have received a lot of attention over the past few years. Due to their unique morphologies and remarkable optical and physiochemical properties, they have been widely explored in imaging, drug delivery and cancer treatments.[3–5] However, their promise as a gene delivery system for the treatment of cancer has only been revealed so far in association with photothermal therapy and chemotherapeutics.[6–8] Recently, we have demonstrated that lactoferrin-conjugating gold nanocages induced gene expression in PC-3 prostate cancer cell line without the help of any external stimulation.[9] Hence, the aim of this work is to further investigate whether conjugating the targeting ligand lactoferrin and the diaminobutyric polypropylenimine

Received: 7 January 2022
Accepted: 1 March 2022
Published: 25 March 2022

Graphical Abstract

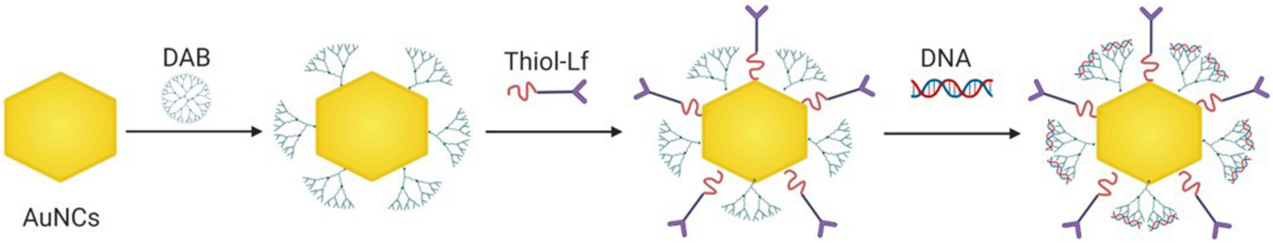

dendrimer onto the surface of gold nanocages, followed by complexation with therapeutic DNA, would enhance the anti-proliferation activity in a prostate cancer cell line without the use of external stimulation. Generation 3- diaminobutyric polypropylenimine (DAB) dendrimer has been shown to have great potential for gene delivery applications due to its ability to condense DNA and its high gene expression efficacy.[10–12] We previously demonstrated that novel intravenously administered lactoferrin-bearing DAB dendriplexes improved tumor gene expression, while decreasing non-specific gene expression in the liver.[10] Furthermore, the intravenous administration of lactoferrin-bearing, TNFα-encoding dendriplexes led to a sustained inhibition of tumor growth and even tumor suppression for 40% of the A431 epidermoid carcinoma tumors and up to 50% of the B16-F10 melanoma tumors, with long-term survival of the animals.[10] In contrast, 100% of the tumors treated with naked DNA or left untreated were progressive. The animals did not show any signs of toxicity.

Plasmid DNA encoding TNFα, an inflammatory cytokine, was chosen for this study because of its well-known strong ability to induce apoptosis in various cancer cell lines, and particularly in prostate cancer cells.[13–15] We previously demonstrated that the intravenous administration of transferrin-bearing DAB dendriplex encoding TNFα resulted in tumor suppression for 60% of PC-3 and 50% of DU145 prostate tumors.[14] The survival of the treated mice was increased by 22 days compared to untreated tumors, for both cell lines. In another study, the intravenous administration of lactoferrin-bearing DAB dendriplexes encoding TNFα resulted in the complete suppression of 70% of PC-3 and 50% of DU145 tumors over one month, with long-term survival of the mice.[15] By contrast, all the tumors treated with the dendrimer, with naked DNA or left untreated, were progressive for both tumor types. The animals did not show any signs of toxicity.[15]

The objectives of this study therefore were 1) to synthesize and characterize gold nanocages bearing lactoferrin and conjugated to DAB, 2) to assess the DNA condensation efficiency of this delivery system complexed with a plasmid DNA, 3) to evaluate the gene expression efficacy and uptake of the conjugates complexed with DNA by PC-3 prostate cancer cells and 4) to evaluate their anti-proliferative efficacy following complexation with DNA encoding TNFα on PC-3 cells in vitro.

Materials and Methods

Cell Lines and Reagents

Lactoferrin (Lf), generation 3-diaminobutyric polypropylenimine (DAB) dendrimer, chloroauric acid ($HAuCl_4$), silver trifluoroacetate (CF_3COOAg), sodium hydrosulfide hydrate (NaSH), polyvinyl pyrrolidone (PVP, M_w 55,000 Da), diethylene glycol (DEG), sodium chloride (NaCl), aqueous hydrochloric acid solution (HCl, 37%), and deionized (DI) water (resistivity: 18.2 MΩ·cm) were obtained from Sigma Aldrich (Poole, UK). The expression plasmids encoding TNFα (pORF9-mTNFα) and β-galactosidase (pCMVsport β-galactosidase) were respectively purchased from InvivoGen (San Diego, USA) and Invitrogen (Paisley, UK). N-[1-(2,3-Dioleoyloxy) propyl]-N,N,N-trimethylammonium methyl-sulfate (DOTAP) came from Roche (Burgess Hill, UK).

Passive lysis buffer was obtained from Promega (Southampton, UK). Label IT® Fluorescein Nucleic Acid Labelling Kit and Vectashield® mounting medium containing 4′,6-diamidino-2-phenylindole (DAPI), respectively, came from Cambridge BioSciences (Cambridge, UK) and Vector Laboratories (Peterborough, UK). Bioware® androgen-irresponsive PC-3M-luc-C6 human prostate adenocarcinoma expressing luciferase was obtained from Caliper Life Sciences (Hopkinton, MA). Minimum Modified Eagle's Medium (MEM), L-glutamine, fetal bovine serum (FBS) and penicillin-streptomycin were purchased from Life Technologies (Paisley, UK).

Synthesis of Gold Nanocages Conjugates

Preparation of Thiolated DAB Dendrimer

A thiolated generation 3-DAB dendrimer was prepared with modifications from a previously published method.[16] The DAB dendrimer was thiolated by mixing with an excess of 2-fold moles of Traut's reagent (2-iminothiolane). To do so, Traut's reagent (3.44 mL, 3.44 mg/mL in PBS, 25 mM) was added to DAB solution (3.44 mL, 21.08 mg/mL in PBS, 12.5 mM) and vortexed for 5 seconds. The reaction mixture was then incubated at 25°C for 24 hours. The purification of the thiolated dendrimer was done at room temperature (20–22°C), using benzoylated dialysis tubing (MWCO: 2000 Da) against 2 L of distilled water, which was changed twice in 24 h. The dialyzed solution of the final compound was then freeze-dried using a Christ Epsilon 2–4 LSC® freeze dryer (Osterode am Harz, Germany) for 48 hours.

Preparation of Lactoferrin-Bearing Dendrimer-Conjugated Gold Nanocages

Gold nanocages (AuNCs) and thiolated Lf were prepared as previously described.[9] Thiolated-DAB (240 µL, 7.26 mg/mL in PBS) was added to each of the 1 mL as-prepared AuNCs, then mixed by vortexing for 5 seconds and incubated at a temperature of 25°C for 24 hours. AuNCs-DAB was then purified twice with DI water (1 mL), using a Vivaspin-6® centrifuge tube (MWCO: 5000 Da) at 8000 rpm (14,000 g) for 20 minutes. As-prepared thiolated Lf (100 µL, 8 mg/mL) was then added to each 1 mL of AuNCs-DAB to prepare AuNCs-DAB-Lf conjugates, vortexed and incubated for 24 hours at 25°C. The AuNCs-DAB-Lf conjugates were then purified twice with DI water (1 mL), using a Vivaspin-6® centrifuge tube (MWCO: 100,000 Da) at 8000 rpm (14,000 g) for 20 minutes. The purified conjugates were finally freeze-dried for 48 hours using a Christ® freeze dryer.

Characterization of Gold Nanocages Conjugates

UV-Vis Spectrometry Analysis

The synthesis of the AuNCs conjugates was analyzed by UV-Vis spectrometry, in the wavelength range of 300–900 nm, using a Varian Cary® 50 Bio UV-visible spectrophotometer. The spectrum of DI water was adjusted as baseline before measuring the samples.

Size and Zeta Potential Measurement

The size of AuNCs conjugates in DI water was determined by photon correlation spectroscopy, while their zeta potential was measured by laser Doppler electrophoresis, using a Malvern Zetasizer Nano-ZS® (Malvern Instruments, Malvern, UK) at 25°C. These measurements were conducted in triplicate, with a scattering angle of 173° and He–Ne laser operating at 632.8 nm.

Characterization of AuNCs-DAB-Lf-DNA Complexes

Gel Retardation Assay

The condensation of DNA to AuNCs-DAB-Lf was determined by agarose gel retardation assay. AuNCs-DAB-Lf complexes were prepared at AuNCs-DAB-Lf: DNA weight ratios ranging from 0.5:1 to 40:1, while the DNA concentration was maintained constant at 20 µg/mL. (This concentration was higher than the one used for the determination of the size and zeta potential of AuNCs-DAB-Lf complexes, to facilitate the examination of the partial or full condensation of DNA to AuNCs-DAB-Lf). Following mixing with the loading buffer, the samples (15 µL) were loaded on a 1X Tris-Borate-EDTA (TBE) (Tris base (89 mM), boric acid (89 mM) and Na_2-EDTA (2 mM) at pH 8.3)- buffered agarose gel (0.8% w/v) containing ethidium bromide (0.4 µg/mL). TBE (1x) was used as a running buffer. The DNA size marker used in this experiment was HyperLadder I. The gel was run for 1 h at 50 V and then photographed under UV light.

Size and Zeta Potential of AuNCs-DAB-Lf-DNA Complexes

The size and zeta potential of AuNCs-DAB-Lf complexes in 5% (w/v) glucose solution were determined for AuNCs-DAB-Lf: DNA weight ratios ranging from 0.5:1 to 40:1, as described above. The DNA concentration was maintained constant at 1 μg/mL.

In vitro Biological Characterization

Cell Culture

PC-3 prostate cancer cells were grown in Minimum Modified Eagle's Medium (MEM) supplemented with 10% (v/v) fetal bovine serum, 1% (v/v) L-glutamine, and 0.5% (v/v) penicillin–streptomycin. The cells were kept at 37°C in a 5% carbon dioxide humid atmosphere.

Gene Expression

The gene expression efficacy of DNA complexed to AuNCs-DAB-Lf was evaluated using a β-galactosidase quantification assay. The cells were seeded in 96-well plates at a concentration of 10,000 cells/well and incubated at 37°C for 24 h in a 5% CO_2 atmosphere. They were then treated with AuNCs-DAB-Lf complexed to plasmid DNA encoding β-galactosidase, at various AuNCs-DAB-Lf: DNA weight ratios (40:1, 20:1, 10:1, 5:1, 2:1, 1:1, and 0.5:1), in quintuplicate. DOTAP-DNA (optimal weight ratio 5:1) and DAB-DNA (optimal weight ratio 5:1) were used as positive controls, whereas naked DNA served as a negative control. The plasmid concentration (0.5 μg/well) was maintained constant throughout the experiment. The treated cells were incubated for 72 h before analysis. They were then lysed for 20 min with passive lysis buffer (PLB) (1X, 50 μL/well) and then tested for β-galactosidase expression.[17] To do so, 50 μL of the assay buffer (1.33 mg/mL o-nitrophenyl- β-D-galactosidase, 100 mM mercaptoethanol, 2 mM magnesium chloride, 200 mM sodium phosphate buffer, pH 7.3) was added to each well containing the lysates. Following the incubation of the lysed cells at 37°C for 2 h, the absorbance of the samples was read at 405 nm using a Multiskan Ascent® plate reader (MTX Lab Systems, Bradenton, FL).

Cellular Uptake

The cellular uptake of DNA complexed with AuNCs-DAB-Lf was quantified by flow cytometry. Plasmid DNA was labelled with the fluorescent probe fluorescein using a Label IT® Fluorescein Nucleic Acid Labeling kit, as described by the manufacturer. PC-3 cells were seeded in 6-well plates at a density of 3×10^5 cells per well and grown at 37°C for 24 h, before being treated with fluorescein-labelled DNA (2.5 μg DNA per well), alone or complexed with AuNCs-DAB-Lf (at AuNCs-DAB-Lf: DNA weight ratios of 10:1 and 20:1) and DAB (at a dendrimer: DNA weight ratio of 5:1). Untreated cells served as a negative control. Following incubation with the treatments for 24 h, each well was washed with PBS (2 mL, pH 7.4) twice. Single-cell suspensions were then prepared by using trypsin (250 μL per well), and then medium (500 μL per well) once the cells were detached, before analysis with a FACSCanto® flow cytometer (BD, Franklin Lakes, NJ). Their mean fluorescence intensity was determined with FACSDiva® software (BD, Franklin Lakes, NJ), counting 10,000 cells (gated events) for each sample.

Confocal microscopy was also used to qualitatively assess the cellular uptake of DNA complexed with AuNCs-DAB-Lf. PC-3 cells were seeded at a concentration of 3×10^5 cells per well on coverslips in 6-well plates and grown at 37°C for 24 h. The cells were then treated with fluorescein-labelled DNA (2.5 μg/well) complexed to AuNCs-DAB-Lf (weight ratio: 10:1) and DAB (dendrimer: DNA weight ratio of 5:1) at 37°C for 24 h. Control wells were also treated with naked DNA or left untreated. Following treatment, the cells were washed with PBS (3 mL) twice, fixed with methanol (2 mL) at 20°C for 10 min, and washed again with PBS (3 mL). Upon staining of the nuclei with Vectashield® mounting medium containing DAPI, the cells were examined using a Leica TCS SP5 confocal microscope (Wetzlar, Germany). DAPI (which stained the cell nuclei) was excited with a 405 nm laser line (emission bandwidth: 415–491 nm) and fluorescein (labelling the DNA) was excited with a 514 nm laser line (emission bandwidth: 550–620 nm).

Anti-Proliferative Activity

The anti-proliferative activity of AuNCs-DAB-Lf complexed with plasmid DNA encoding TNFα was evaluated using an MTT assay. PC-3 cells were seeded in 96-well plates at a density of 10,000 cells/well, in quintuplicate, and incubated for 24 h at 37°C. They were then treated with the AuNCs-DAB-Lf complexes at AuNCs-DAB-Lf: DNA weight ratios of 10:1 and 40:1 using various DNA concentrations (from 80 to 0.31 μg/mL and 20 to 0.08 μg/mL, respectively). Naked

DNA served as a negative control, while DAB:DNA at a 5:1 ratio was used as a positive control. The cytotoxicity of the prepared AuNCs-DAB-Lf conjugates was also examined by the same method, treating the seeded cells with 800 to 3.12 µg/mL, which is equivalent to the amount of AuNCs-DAB-Lf used in the anti-proliferation assay. The plates were incubated at 37°C and 5% CO_2 for 72 h, then 50 µL of MTT solution (0.5%) was added to each well. Following a 4-h incubation at 37°C with protection from light, the medium was then replaced with DMSO (200 µL per well) to dissolve the precipitated formazan. The absorbance of the complex was measured at 570 nm using a plate reader (Thermo Labsystems, Multiskan Ascent®). The growth inhibitory concentration for 50% of the cells (IC_{50}) was determined by plotting a dose–response curve between the percentage of the cell viability and the logarithm of the DNA concentration.

Statistical Analysis

Results were expressed as means ± standard error of the mean (SEM). Statistical significance was determined by using one-way analysis of variance (ANOVA), followed by Tukey multiple comparison post-test (Minitab® software, State College, PE). Differences were considered statistically significant for P values lower than 0.05.

Results

Characterization of Gold Nanocages Conjugates

UV-Vis-spectrometry analysis confirmed the conjugation of DAB and Lf onto the surface of AuNCs (Figure 1). Gold conjugates displayed UV-vis spectrum peaks in the near-infrared (NIR) regions (respectively 715 nm, 745 nm and 757 nm for AuNCs, AuNCs-DAB-Lf and AuNCs-DAB). The surface modification of AuNCs with DAB and Lf was confirmed by the red-shift in the UV-vis spectra of AuNCs-DAB-Lf compared to that of the unmodified AuNCs.

The size and zeta potential of the unmodified AuNCs and AuNCs conjugates were measured to assess the formation of AuNCs conjugates. Conjugating DAB and Lf onto AuNCs induced a slight increase in the size of AuNCs-DAB-Lf (92.65 ± 0.57 nm, polydispersity index (PDI):0.261) in comparison with AuNCs (88.69 ± 0.66 nm, PDI: 0.204). Zeta

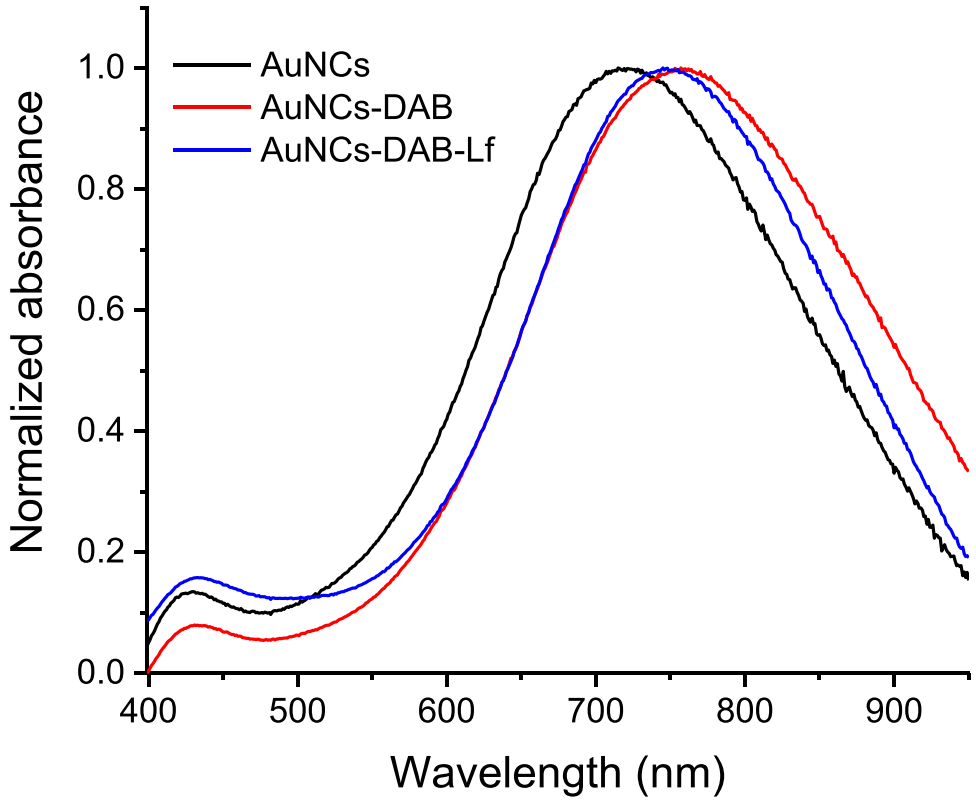

Figure 1 UV-vis spectra of AuNCs, AuNCs-DAB and AuNCs-DAB-Lf.

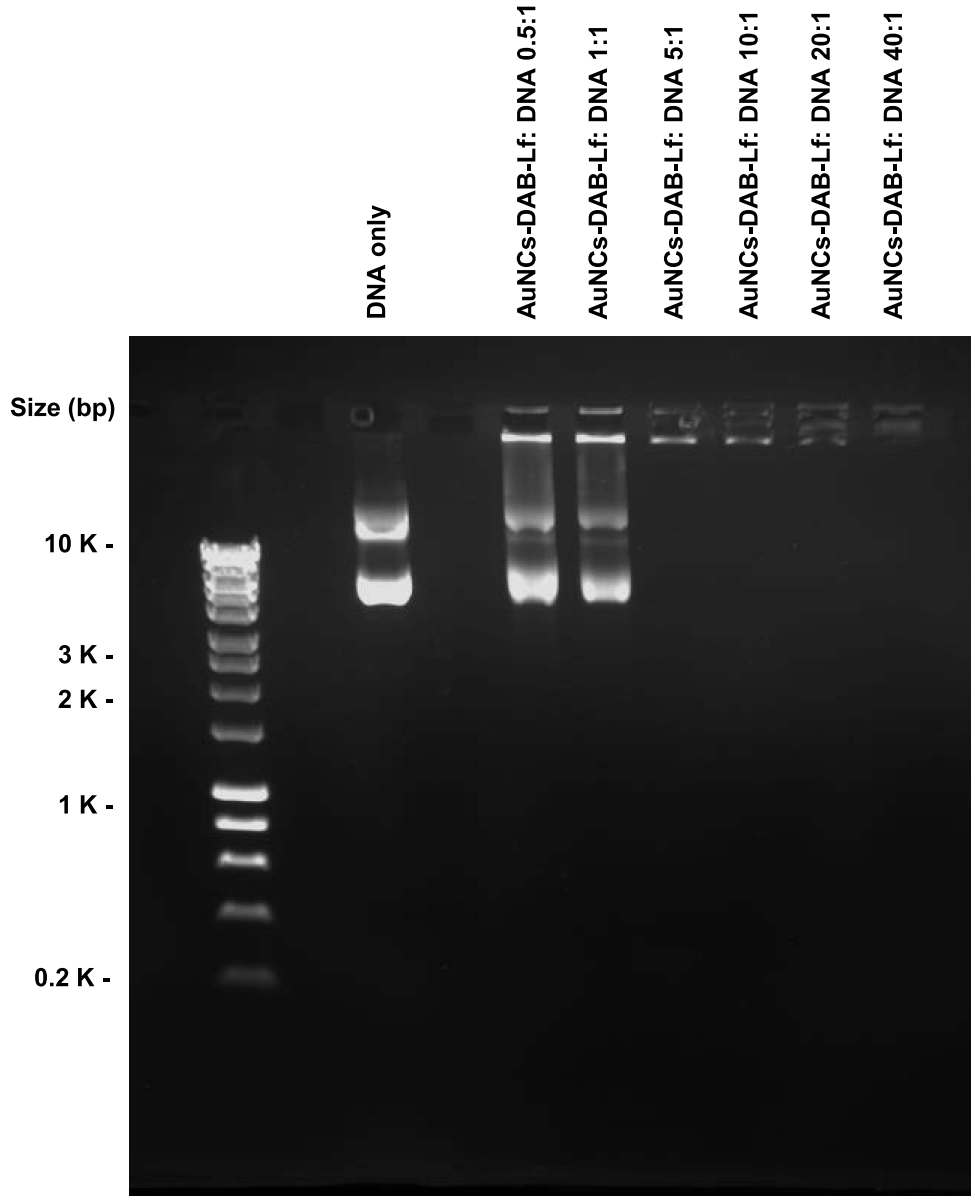

Figure 2 Gel retardation assay of AuNCs-DAB-Lf-DNA complex at various AuNCs-DAB-Lf: DNA weight ratios (0.5:1, 1:1, 5:1, 10:1, 20:1, 40:1) (control: DNA only).

potential measurements revealed the change in AuNCs surface charge upon conjugation with DAB and Lf. The surface charge of AuNCs changed from a highly negative potential (−20.50 ± 0.38 mV) for unmodified AuNCs to positive potentials (respectively 25 ± 0.52 mV and 13.80 ± 0.18 mV for AuNCs-DAB and AuNCs-DAB-Lf).

Characterization of AuNCs-DAB-Lf-DNA Complexes

Gel Retardation Assay

The DNA condensation by AuNCs-DAB-Lf was confirmed by a gel retardation assay. The plasmid DNA was fully condensed at AuNCs-DAB-Lf: DNA weight ratios of 5:1 and above. Ethidium bromide could not intercalate with DNA, and no band corresponding to free DNA was visible at these ratios (Figure 2). However, DNA was partially condensed at AuNCs-DAB-Lf: DNA weight ratios of 1:1 and below, and a band corresponding to free DNA was therefore visible.

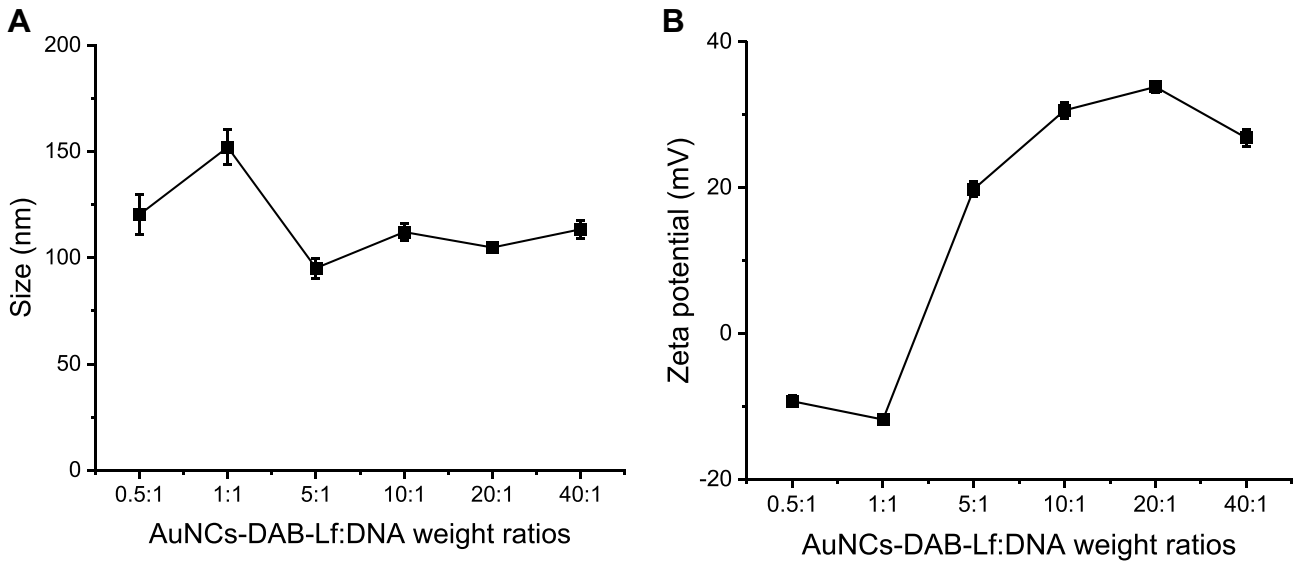

Figure 3 Size (**A**) and zeta potential (**B**) of AuNCs-DAB-Lf complexed with DNA at various AuNCs-DAB-Lf: DNA weight ratios. Results are expressed as mean ± SEM (n = 9) (error bars smaller than symbols).

Size and Zeta Potential of AuNCs-DAB-Lf-DNA Complexes

AuNCs-DAB-Lf complexed with DNA had an average size smaller than 160 nm at all AuNCs-DAB-Lf: DNA weight ratios used (Figure 3A). Their size decreased with an increase in the weight ratios, from 1:1 to 5:1, before reaching a plateau at a AuNCs-DAB-Lf: DNA weight ratio of 10:1 onwards, indicating the formation of more compact complexes between AuNCs-DAB-Lf and DNA. AuNCs-DAB-Lf-DNA exhibited its largest size (152 ± 8.24 nm) at a weight ratio of 1:1 and its smallest size (95.11 ± 4.78 nm) at weight ratio at 5:1.

AuNCs-DAB-Lf complexes displayed negative surface charges of −9.28 ± 0.72 mV and −11.80 ± 0.34 mV at the minimum weight ratios of 0.5:1 and 1:1, respectively, indicating that the negatively charged plasmid DNA was not fully complexed with AuNCs-DAB-Lf at these ratios. The surface charge then increased as the weight ratios of the complexes increased, to finally reach a positive charge (26.80 ± 1.18 mV) at the weight ratio of 40:1 (Figure 3B).

In vitro Biological Characterization

Gene Expression

The treatment of PC-3 cancer cells with AuNCs-DAB-Lf complexed with plasmid DNA induced gene transfection at weight ratios of 5:1, 10:1 and 20:1 (Figure 4). The highest gene expression level was obtained following treatment with AuNCs-DAB-Lf-DNA at a weight ratio of 10:1 (3.44 ± 0.23 mU/mL). At this ratio, the gene expression efficacy was 3-fold higher than when treated with DNA (1.16 ± 0.01 mU/mL), 2.1-fold higher than with treatment with DOTAP (1.68 ± 0.09 mU/mL) and 1.9-fold higher than what observed with DAB (1.85 ± 0.08 mU/mL).

Cellular Uptake

The treatment of PC-3 prostate cancer cells with AuNCs-DAB-Lf complexed with fluorescein-labelled DNA at a weight ratio of 10:1 led to the highest fluorescence in the cells (6896.33 ± 353.48 arbitrary units (a.u.)) (Figure 5). This cellular fluorescence was 1.5-fold and 35.6-fold higher than that observed as a result of treatment with DAB (4517.33 ± 152.27 a.u.) and DNA solution (199.50 ± 1.31 a.u.), respectively. Furthermore, the treatment with naked DNA led to a weak cellular uptake, highlighting the failure of plasmid DNA to be taken up by PC-3 prostate cancer cells without the assistance of a delivery system.

The uptake of fluorescein-labelled DNA complexed with AuNCs-DAB-Lf by PC-3 prostate cancer cells was also qualitatively confirmed by confocal microscopy (Figure 6). Fluorescein-labeled DNA was disseminated in the cytoplasm following treatment with AuNCs-DAB-Lf-DNA and DAB-DNA dendriplex. The DNA uptake appeared to be more

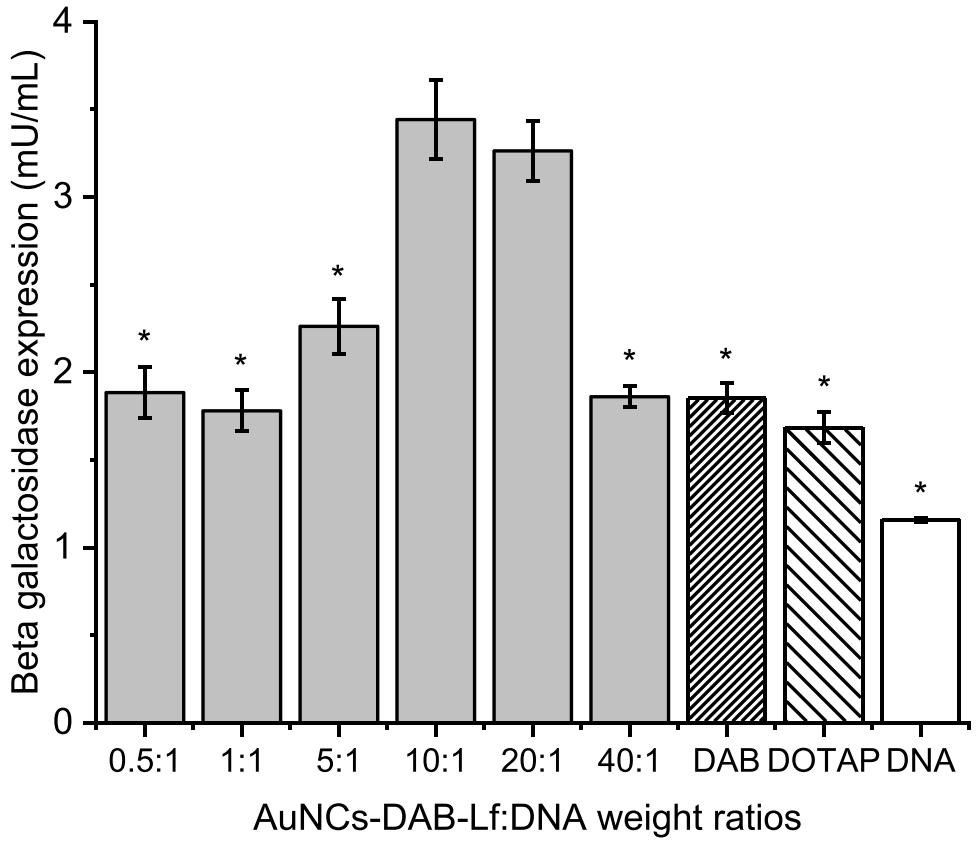

Figure 4 Transfection efficiency of AuNCs-DAB-Lf at various AuNCs-DAB-Lf: DNA weight ratios in PC-3 cells. Results are expressed as the mean ± SEM of three replicates (n=*15*). **P < 0.05* versus the highest transfection ratio.

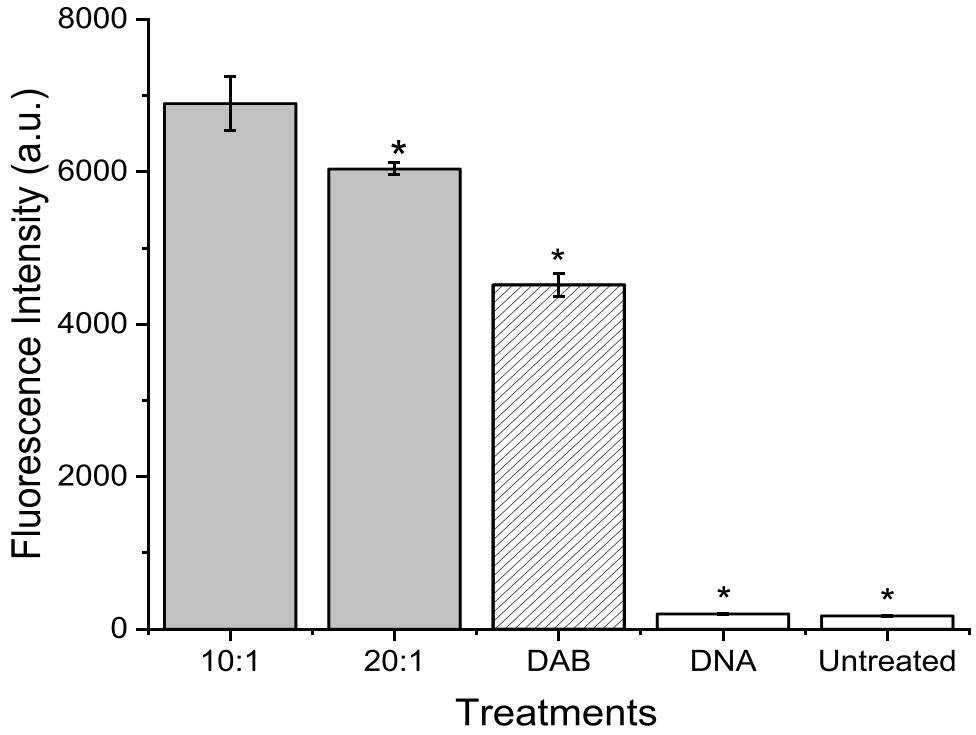

Figure 5 Quantification of the cellular uptake of fluorescein-labelled DNA complexed with AuNCs-DAB-Lf or left uncomplexed, after 24 h incubation with PC-3 cells, using flow cytometry (n = *6) (*P < 0.05* versus the highest fluorescence intensity).

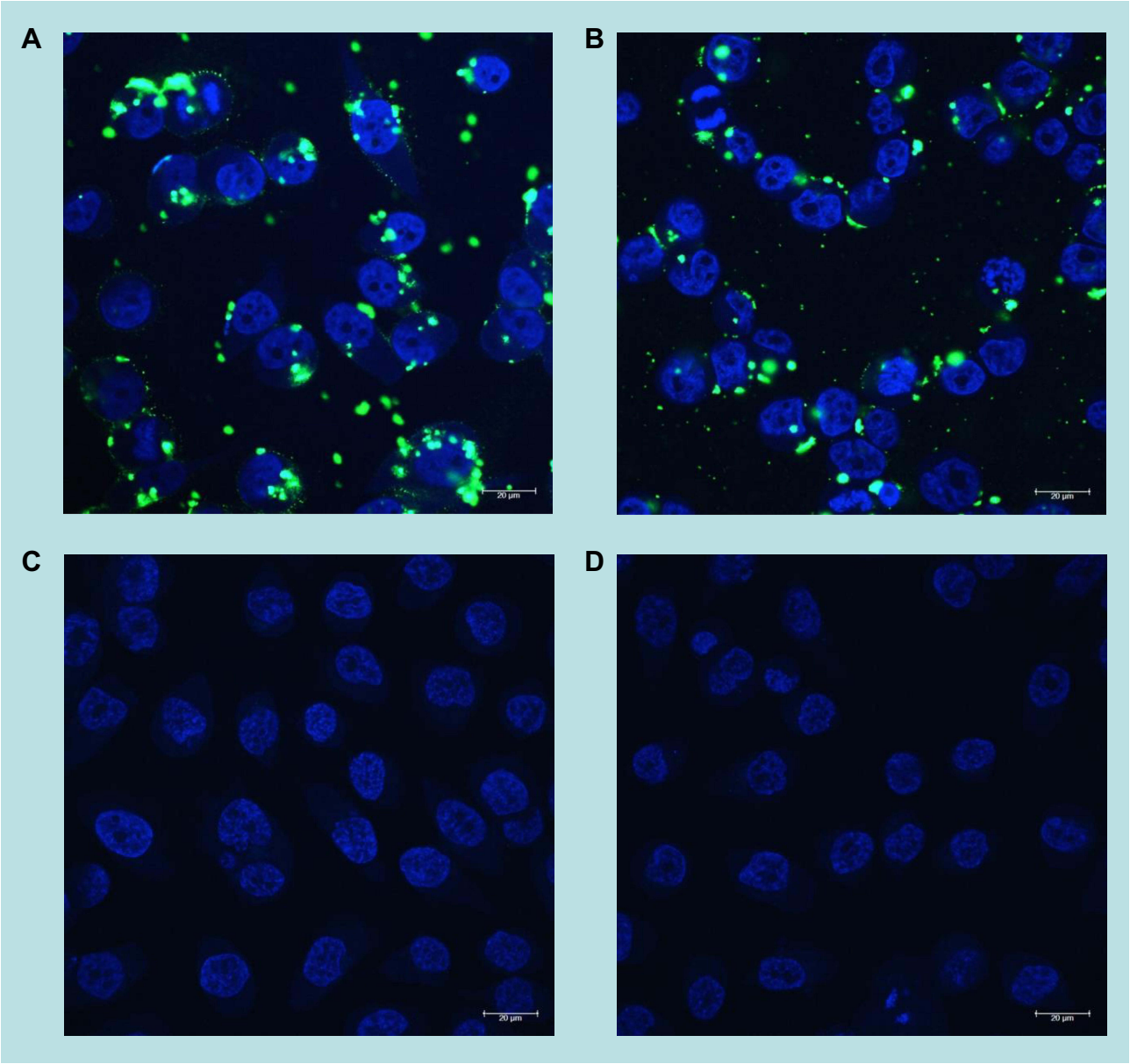

Figure 6 Confocal microscopy images of the cellular uptake of fluorescein-labelled DNA (2.5 µg per well), complexed with (**A**) AuNCs-DAB-Lf at weight ratio of 10:1, (**B**) DAB with weight ratio of 5:1, (**C**) free in solution after 24 h incubation with PC-3 cells ((**D**) untreated cells). Blue: nuclei stained with DAPI (excitation: 405 nm laser line; bandwidth: 415–491 nm), green: fluorescein-labelled DNA (excitation: 453 nm laser line; bandwidth: 550–620 nm) (magnification: ×63).

pronounced in the cancer cells treated with AuNCs-DAB-Lf complex than following treatment with DAB dendriplex. DNA did not co-localize in the nuclei after this duration of treatment. In contrast, the cells treated with DNA solution did not display any fluorescein-derived fluorescence.

Anti-Proliferative Activity

The treatment of PC-3 prostate cancer cells with AuNCs-DAB-Lf complexed with DNA encoding TNFα at the weight ratios of 40:1 and 10:1 induced an increase in the in vitro anti-proliferative efficacy, respectively, by 9- and 2.4-fold, with an IC_{50} of 1.80 ± 0.31 and 6.66 ± 1.87 µg/mL compared with the positive control DAB dendriplex (IC_{50}: 16.28 ± 1.31 µg/mL) (Figure 7A and B).

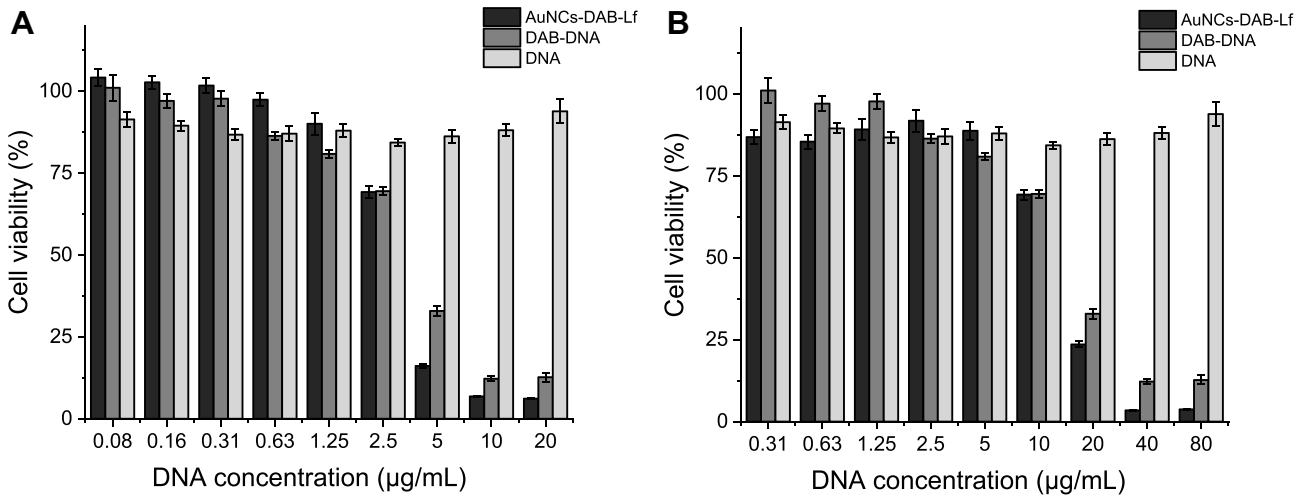

Figure 7 Anti-proliferative activity of AuNCs-DAB-Lf complexed with DNA-encoding TNFα at conjugate: DNA weight ratio of 40:1 (**A**) and 10:1 (**B**) in PC-3 cells (*n = 15*).

Discussion

The use of gold nanocages as gene delivery systems for the treatment of cancer has previously been reported jointly with chemotherapeutics and photothermal therapy, but not without external triggers so far. To explore this possibility, we hypothesize that the grafting of the tumor-targeting ligand lactoferrin and the cationic dendrimer DAB on gold nanocages complexed with plasmid DNA would lead to an increased cellular uptake, gene expression and anti-proliferative activity in PC-3 cancer cells. Lactoferrin and DAB were conjugated to the surface of gold nanocages through gold-thiolate (Au-S) bonds, thus generating positively charged gold conjugates able to condense negatively charged plasmid DNA through electrostatic interactions.

The surface modification of the gold nanocages with Lf and DAB was analyzed by UV-vis spectroscopy. The surface plasmon resonance of AuNCs-DAB-Lf was 745 nm upon surface functionalization of AuNCs with Lf and DAB. The red-shifted absorption peaks of AuNCs-DAB-Lf, compared with the unmodified AuNCs, are attributed to the change in refractive index on the AuNCs surface. This confirmed the surface functionalization and further indicated that the shape and structure of the nanocages remained the same upon the functionalized conjugation.[6] AuNCs-DAB-Lf conjugates exhibited UV-Vis spectra peaks in the near-infrared region (700–900 nm), which makes them suitable for potential photothermal and imaging applications.

Conjugating DAB and Lf to AuNCs resulted in an enhanced transfection level at the optimum weight ratio of 10:1 by 1.9- and 2.1-fold compared to DAB and DOTAP polyplexes, respectively, and these results corroborate other reported studies. For instance, Ghosh and colleagues demonstrated that lysine dendrimer-functionalized gold nanoparticles efficiently condensed the DNA and significantly enhanced β-galactosidase gene expression by 28-fold in Cos-1 monkey kidney cells in comparison with what was observed after treatment with the positive control polylysine.[18] Kim and colleagues also demonstrated that dendron-conjugated gold nanoparticles improved gene silencing by 48% at an NP/siRNA ratio of 2, for which the siRNA was fully complexed, and showed therefore a knockdown efficiency similar to that obtained from positive control Lipofectamine® in SVR-bag4 endothelial cells.[19]

In this study, the increase of β-galactosidase expression following the treatment of the cells with AuNCs-DAB-Lf complexes most likely resulted from the higher zeta potential of these complexes due to the strong correlation between the positive charge density of the complexes and their cellular uptake.[20]

Furthermore, the presence of gold nanocages in AuNCs-DAB-Lf could also play a role in improving their β-galactosidase expression compared to DAB and DOTAP polyplexes. This improvement in gene expression could be attributed to the presence of rigid gold nanoparticles in gene carriers that 1) preserved the 3D structures of the attached polymers, enabling the high condensation of DNA into small complexes, 2) promoted the mono-dispersity of these complexes, and 3) facilitated DNA internalization into the cells, consequently resulting in enhanced gene transfection

more than that obtained from polyplexes.[21,22] Also, this may be because the complexed DNA could be easily released from the gold conjugate following internalization by the cell, whereas the DNA would be tightly condensed by the polyplex, thereby making its disassociation from the polyplex and release within the cells more difficult.[23] The shape of nanoparticles is another factor that may affect gene delivery efficiency and cell internalization. Morgan and colleagues investigated the effect of the shape of three gold nanoparticle formulations (nanocages, nanoshells and nanorods) that covalently attached to thiol-siRNA in HeLa cells under NIR laser irradiation.[24] They demonstrated that both gold nanocages and nanoshells displayed high knockdown efficiency with high particle concentrations, demonstrating the efficient internalization of gold nanocages and nanoshells into HeLa cells compared to that observed from gold nanorods. It was found that doubling the particle concentration of nanorods induced a 2-fold enhancement of green fluorescent protein (GFP) knockdown efficacy, demonstrating the need for a larger amount of nanorod particles to induce a similar GFP knockdown level to that observed for the nanocages and nanoshells. These findings highlighted the importance of cage shape when using gold nanoparticles as a gene delivery system by showing the strong impact of the gold nanoparticle shape on cellular internalization and therefore on the efficiency of gene expression.

The cellular uptake of the DNA complexed to AuNCs-DAB-Lf was significantly higher than that observed with the positive control DAB dendriplex. The structure and unique morphology of gold nanocages could contribute to the enhancement of cellular uptake over other types of nanoparticles. Robinson and colleagues found that gold nanocages were taken up by DU145 prostate cancer cells 28% more than gold nanorods.[25] They were also taken up by HUVEC human umbilical vein endothelial cells 18% more than the nanorods. These findings indicate that the shape of gold nanocages could play a pivotal role in facilitating their uptake in prostate cancer cells as well as in healthy cells. In this study, the high cellular uptake of AuNCs-DAB-Lf complex over the positive control DAB dendriplex could also be attributed to the rigid structure of gold nanoparticles, which has been reported to enhance cellular uptake compared to delivery systems bearing softer structures, such as liposomes and polymeric nanoparticles.[26] Liu and colleagues previously studied the role of nanoparticle rigidity on cellular uptake using G5 dendrimers as soft nanoparticles and dendrimers-coated gold nanoparticles as rigid nanoparticle models.[27] They found that the uptake of dendrimer-coated gold nanoparticles was 3.2-fold higher than that observed from dendrimers in both U87MG cancer cells and L929 healthy cells. As the adsorption and cellular uptake of nanoparticles depend on their shape, surface modifications, size and charge, the enhanced cellular uptake of the gold conjugates could also be due to the cationic polymer modification on the gold nanocages and the positive charge of gold complexes. Cho and colleagues demonstrated that PAA-coated gold nanocages, which had a positive charge of +15.9 ± 2.7 mV, were taken by SK-BR-3 BC cells in larger amounts than negatively charged gold nanocages modified with anti-HER2 antibody (−2.7 ± 4.9 mV) and polyethylene glycol (PEG)-modified gold nanocages (−2.0 ± 5.4 mV).[28]

AuNCs-DAB-Lf complexed with DNA encoding TNFα enhanced the anti-proliferative activity by 9-fold compared to DAB dendriplex. These findings could be attributed to improved gene expression efficacy and efficient cellular uptake followed by treatment with AuNCs-DAB-Lf complex. Further, the cytotoxicity results of AuNCs-Lf complexes indicated that the therapeutic effect achieved could be attributed to the efficient delivery of the therapeutic gene, as AuNCs-Lf conjugates demonstrated a minimum cytotoxicity effect.[9] In a previous study, we found that Lf-conjugated DAB (DAB-Lf) dendriplex encoding TNFα led to improved anti-proliferative activity by 1.9-fold in PC-3 cancer cells in comparison with non-conjugated DAB dendriplex.[15] Therefore, the higher anti-proliferative activity of AuNCs-DAB-Lf complex over DAB-Lf dendriplex compared with DAB dendriplex indicates the importance of AuNCs in improving gene therapeutic effect due to the crucial role of AuNCs in enhancing cellular uptake and transfection efficacy.

Conclusion

This study revealed that novel lactoferrin-bearing DAB-conjugated gold nanocages were able to complex with plasmid DNA at conjugate: DNA weight ratios of 5:1 and above. These results were translated in vitro into higher DNA transfection compared to the positive controls DAB and DOTAP polyplexes in PC-3 prostate cancer cells. This was probably a consequence of the increase in the DNA uptake by these cells treated with this complex, in comparison with what was observed following treatment with DAB dendriplex. This further resulted in an increased anti-proliferative activity of therapeutic plasmid DNA encoding TNFα by up to 9-fold when complexed with AuNCs-DAB-Lf, compared

to DAB dendriplex encoding TNFα. This anti-proliferative activity was much enhanced compared to the 1.9-fold improvement reported when treating PC-3 prostate cancer cells with Lf-conjugated DAB dendriplex encoding TNFα. To our knowledge, this is the first time that lactoferrin-bearing gold nanocage-dendrimer conjugates have been used to target cancer cells, leading to increased DNA uptake, gene expression and anti-proliferative activity, without involving any external stimulation. Lactoferrin-bearing gold nanocages-dendrimer conjugates are therefore promising nanocarriers for gene-based prostate cancer therapy and will be further investigated, either alone or synergistically with other cancer therapies.

Abbreviations

ANOVA, one-way analysis of variance; AuNCs, gold nanocages; AuNCs-DAB, AuNCs gold nanocages conjugated to generation 3-diaminobutyric polypropylenimine dendrimer; AuNCs-DAB-Lf, lactoferrin-bearing AuNCs gold nanocages conjugated to generation 3-diaminobutyric polypropylenimine dendrimer; Au-S, gold-thiolate bond; CF_3COOAg, silver trifluoroacetate; DAB, generation 3-diaminobutyric polypropylenimine dendrimer; DAPI, 4′,6-diamidino-2-phenylindole; DEG, diethylene glycol; DI, deionized water; DMSO, dimethyl sulfoxide; DNA, deoxyribonucleic acid; DOTAP, N-[1-(2,3-Dioleoyloxy) propyl]-N,N,N-trimethylammonium methylsulfate; FBS, fetal bovine serum; GFP, green fluorescent protein; $HAuCl_4$, chloroauric acid; HCl, hydrochloric acid; Lf, lactoferrin; MEM, modified Eagle medium; MWCO, molecular weight cut-off; NaCl, sodium chloride; NaSH, sodium hydrosulfide hydrate; PBS, phosphate buffer saline; PEG, polyethylene glycol; PLB, passive lysis buffer; PVP, polyvinyl pyrrolidone; RNA, ribonucleic acid; S.E.M., standard error of the mean; TBE, Tris-Borate-EDTA; TNFα, tumor necrosis factor-alpha.

Acknowledgments

This work was financially supported by a PhD studentship from the Saudi Arabian Cultural Bureau in the UK and Umm Al-Qura University (Kingdom of Saudi Arabia) to J.A. P.L. is funded by a research grant from Worldwide Cancer Research [grant number 16-1303]. S.S. is funded by a research grant from The Dunhill Medical Trust [grant number R463/0216]. Graphical abstract is created using BioRender.com.

Disclosure

Jamal Almowalad's current affiliation is at the Department of Pharmaceutics, College of Pharmacy, Umm Al-Qura University, Al-Abidiyah, Makkah 21955, Kingdom of Saudi Arabia. Partha Laskar's current affiliation is at the Department of Immunology and Microbiology, University of Texas Health Rio Grande Valley, McAllen, TX 78504, USA. The authors report no conflicts of interest in this work.

References

1. Sung H, Ferlay J, Siegel RL, et al. Global cancer statistics 2020: GLOBOCAN estimates of incidence and mortality worldwide for 36 cancers in 185 countries. *CA: Cancer J Clin*. 2021;71:209–249.
2. Graff JN, Chamberlain ED. Sipuleucel-T in the treatment of prostate cancer: an evidence-based review of its place in therapy. *Core Evid*. 2015;10:1–10.
3. Skrabalak SE, Chen J, Sun Y, et al. Gold nanocages: synthesis, properties, and applications. *Acc Chem Res*. 2008;41:1587–1595.
4. Chen J, Glaus C, Laforest R, et al. Gold nanocages as photothermal transducers for cancer treatment. *Small*. 2010;6:811–817.
5. Xia X, Xia Y. Gold nanocages as multifunctional materials for nanomedicine. *Front Phys*. 2014;9:378–384.
6. Huang S, Duan S, Wang J, et al. Folic-acid-mediated functionalized gold nanocages for targeted delivery of anti-miR-181b in combination of gene therapy and photothermal therapy against hepatocellular carcinoma. *Adv Funct Mater*. 2016;26:2532–2544.
7. Huang S, Liu Y, Xu X, et al. Triple therapy of hepatocellular carcinoma with microRNA-122 and doxorubicin co-loaded functionalized gold nanocages. *J Mater Chem B*. 2018;6:2217–2229.
8. Zhang H, Gao Z, Li X, et al. Multiple-mRNA-controlled and heat-driven drug release from gold nanocages in targeted chemo-photothermal therapy for tumors. *Chem Sci*. 2021;12:12429–12436.
9. Almowalad J, Somani S, Laskar P, et al. Lactoferrin-bearing gold nanocages for gene delivery in prostate cancer cells in vitro. *Int J Nanomedicine*. 2021;16:4391–4407.
10. Lim LY, Koh PY, Somani S, et al. Tumor regression following intravenous administration of lactoferrin-and lactoferricin-bearing dendriplexes. *Nanomedicine*. 2015;11:1445–1454.
11. Somani S, Robb G, Pickard BS, et al. Enhanced gene expression in the brain following intravenous administration of lactoferrin-bearing polypropylenimine dendriplex. *J Control Release*. 2015;217:235–242.

12. Laskar P, Somani S, Campbell SJ, et al. Camptothecin-based dendrimersomes for gene delivery and redox-responsive drug delivery to cancer cells. *Nanoscale*. 2019;11:20058–20071.
13. Aldawsari H, Edrada-Ebel R, Blatchford DR, et al. Enhanced gene expression in tumors after intravenous administration of arginine-, lysine-and leucine-bearing polypropylenimine polyplex. *Biomaterials*. 2011;32:5889–5899.
14. Al Robaian M, Chiam KY, Blatchford DR, et al. Therapeutic efficacy of intravenously administered transferrin-conjugated dendriplexes on prostate carcinomas. *Nanomedicine*. 2014;9:421–434.
15. Altwaijry N, Somani S, Parkinson JA, et al. Regression of prostate tumors after intravenous administration of lactoferrin-bearing polypropylenimine dendriplexes encoding TNF-α, TRAIL, and interleukin-12. *Drug Deliv*. 2018;25:679–689.
16. Liu Y, Chiu GN. Dual-functionalized PAMAM dendrimers with improved P-glycoprotein inhibition and tight junction modulating effect. *Biomacromolecules*. 2013;14:4226–4235.
17. Zinselmeyer BH, Mackay SP, Schätzlein AG, et al. The lower-generation polypropylenimine dendrimers are effective gene-transfer agents. *Pharm Res*. 2002;19:960–967.
18. Ghosh PS, Kim CK, Han G, et al. Efficient gene delivery vectors by tuning the surface charge density of amino acid-functionalized gold nanoparticles. *ACS Nano*. 2008;2:2213–2218.
19. Kim ST, Chompoosor A, Yeh YC, et al. Dendronized gold nanoparticles for siRNA delivery. *Small*. 2012;8:3253–3256.
20. Futaki S, Ohashi W, Suzuki T, et al. Stearylated arginine-rich peptides: a new class of transfection systems. *Bioconjug Chem*. 2001;12:1005–1011.
21. Tencomnao T, Apijaraskul A, Rakkhithawatthana V, et al. Gold/cationic polymer nano-scaffolds mediated transfection for non-viral gene delivery system. *Carbohydr Polym*. 2011;84:216–222.
22. Shan Y, Luo T, Peng C, et al. Gene delivery using dendrimer-entrapped gold nanoparticles as nonviral vectors. *Biomaterials*. 2012;33:3025–3035.
23. Wong SY, Pelet JM, Putnam D. Polymer systems for gene delivery—past, present, and future. *Prog Polym Sci*. 2007;32:799–837.
24. Morgan E, Wupperfeld D, Morales D, et al. Shape matters: gold nanoparticle shape impacts the biological activity of siRNA delivery. *Bioconjug Chem*. 2019;30:853–860.
25. Robinson R, Gerlach W, Ghandehari H. Comparative effect of gold nanorods and nanocages for prostate tumor hyperthermia. *J Control Release*. 2015;220:245–252.
26. Sun J, Zhang L, Wang J, et al. Tunable rigidity of (polymeric core)–(lipid shell) nanoparticles for regulated cellular uptake. *Adv Mater*. 2015;27:402–1407.
27. Liu H, Wang J, Li W, et al. Cellular uptake behaviors of rigidity-tunable dendrimers. *Pharmaceutics*. 2018;10:99–107.
28. Cho EC, Au L, Zhang Q, et al. The effects of size, shape, and surface functional group of gold nanostructures on their adsorption and internalization by cells. *Small*. 2010;6:517–522.